

# Energy loss enhancement of very intense proton beams in dense matter due to the beam-density effect

Benzheng Chen,<sup>1,\*</sup> Jieru Ren,<sup>1,\*</sup> Zhigang Deng,<sup>2,\*</sup> Wei Qi,<sup>2</sup> Zhongmin Hu,<sup>1</sup> Bubo Ma,<sup>1</sup> Xing Wang,<sup>1</sup> Shuai Yin,<sup>1</sup> Jianhua Feng,<sup>1</sup> Wei Liu,<sup>1,3</sup> Zhongfeng Xu,<sup>1</sup> Dieter H. H. Hoffmann,<sup>1</sup> Shaoyi Wang,<sup>2</sup> Quanping Fan,<sup>2</sup> Bo Cui,<sup>2</sup> Shukai He,<sup>2</sup> Zhurong Cao,<sup>2</sup> Zongqing Zhao,<sup>2</sup> Leifeng Cao,<sup>2</sup> Yuqiu Gu,<sup>2</sup> Shaoping Zhu,<sup>2,4,5</sup> Rui Cheng,<sup>6</sup> Xianming Zhou,<sup>1,7</sup> Guoqing Xiao,<sup>6</sup> Hongwei Zhao,<sup>6</sup> Yihang Zhang,<sup>8,9</sup> Zhe Zhang,<sup>8,9</sup> Yutong Li,<sup>8,9</sup> Weimin Zhou,<sup>2,†</sup> and Yongtao Zhao<sup>1,‡</sup>

<sup>1</sup>*MOE Key Laboratory for Nonequilibrium Synthesis and Modulation of Condensed Matter, School of Physics, Xi'an Jiaotong University, Xi'an 710049, China*

<sup>2</sup>*Science and Technology on Plasma Physics Laboratory, Laser Fusion Research Center, China Academy of Engineering Physics, Mianyang 621900, China*

<sup>3</sup>*Xi'an Technological University, Xi'an 710021, China*

<sup>4</sup>*Institute of Applied Physics and Computational Mathematics, Beijing 100094, China*

<sup>5</sup>*Graduate School, China Academy of Engineering Physics, Beijing 100088, China*

<sup>6</sup>*Institute of Modern Physics, Chinese Academy of Sciences, Lanzhou 710049, China*

<sup>7</sup>*Xianyang Normal University, Xianyang 712000, China*

<sup>8</sup>*Beijing National Laboratory for Condensed Matter Physics,*

*Institute of Physics, Chinese Academy of Sciences, Beijing 100190, China*

<sup>9</sup>*School of Physical Sciences, University of Chinese Academy of Sciences, Beijing 100049, China*

(Dated: May 30, 2023)

Thoroughly understanding the transport and energy loss of intense ion beams in dense matter is essential for high-energy-density physics and inertial confinement fusion. Here, we report a stopping power experiment with a high-intensity laser-driven proton beam in cold, dense matter. The measured energy loss is one order of magnitude higher than the expectation of individual particle stopping models. We attribute this finding to the proximity of beam ions to each other, which is usually insignificant for relatively-low-current beams from classical accelerators. The ionization of the cold target by the intense ion beam is important for the stopping power calculation and has been considered using proper ionization cross section data. Final theoretical values agree well with the experimental results. Additionally, we extend the stopping power calculation for intense ion beams to plasma scenario based on Ohm's law. Both the proximity- and the Ohmic effect can enhance the energy loss of intense beams in dense matter, which are also summarized as the beam-density effect. This finding is useful for the stopping power estimation of intense beams and significant to fast ignition fusion driven by intense ion beams.

## I. INTRODUCTION

The energy loss of charged particles in matter has been, and continues to be, a key research topic because of its fundamental importance for a large number of applications such as inertial confinement fusion (ICF) [1–3], medicine [4, 5], and astrophysics [6, 7]. In heavy ion fusion (HIF) [8, 9],  $10^{15}$  Uranium ions at about 10 GeV and compressed into a pulse of 15 ns were supposed to be sufficient for ignition. Even at this intensity theories predicted classical beam transport and classical energy deposition where binary collisions dominate the energy deposition process. Laser-generated proton beams today do even exceed this number in the ps regime. Especially fusion scenarios with fast ignition (FI) depend critically on the energy deposition of intense particle beams in matter [10, 11]. The stopping process of a single charged particle in matter was thoroughly studied by Bethe [12, 13] and Bloch [14]. Subsequently more effort was devoted to theoretical models [15–18] which explained and predicted the energy loss with high precision

for a large existing database [19–21]. Those experiments were performed over a wide range of energies with low-density ion beams from conventional accelerators. The energy loss of individual particles in matter can be well calculated using these models.

Both experimental and theoretical examination have confirmed that the increase of the ion beam density results in orders of magnitude enhancement of beam stopping, compared to the results by individual particle stopping models. Yet there is few practicable models to calculate this enhanced stopping power. Deviations of energy loss from individual particle stopping results were first reported by Brandt, Ratkowski and Ritchie [22], who measured stopping powers for particle clusters of  $H_2^+$  and  $H_3^+$  at energies of  $\sim 100$ -keV/u in carbon and gold. This finding was attributed to what they called the vicinage effect of cluster particles and was caused by the wakes of electron-density fluctuations trailing the ions. This prompted a series of investigations leading to improvement and modification of wake theories [23–26] and the vicinage effect [27–30]. There was also study on the transport of actual high-current charged particles in matter, started with intense electron beams [31–34]. McCorkle and Iafate applied the wake theory and vicinage effect of clusters to dense charged particle beams and proposed the beam-density effect for particle stopping [35].

\* These authors contributed equally to this work.

† zhouwm@caep.cn

‡ zhaoyongtao@xjtu.edu.cn

Another important collective effect on the beam energy loss is the Ohmic loss [36–40], which refers to a decelerating resistive electric field caused by the neutralization of charge and current, in condition of enough free electrons (usually in ionized matter).

Nevertheless, there are still obstacles for the detailed understanding and reliable calculation of energy loss enhancement of intense ion beams in cold targets with few free electrons, in which case the Ohmic effect is weak. The beam-density theory by McCorkle and Iafrate treats the energy loss enhancement from free and bound electrons in the same way, while they should be dealt differently. Additionally, the beam-density theory requires free electrons of non-zero density existing in matter, otherwise it will be invalid due to an infinite result in stopping power calculation. The challenge is to find a proper way to estimate the free electron density of cold matter under intense ion beam impact. A beam-target interaction experiment is also necessary to verify the according results.

In this paper, we report the enhanced stopping power of a cold target for an intense proton beam observed in the experiment. The energy loss of beam protons is measured with high precision and is orders of magnitude higher than the individual particle result, which is attributed to the proximity of beam ions to each other. The local density of free electrons is determined by taking the ionization of the cold target into consideration using proper ionization cross section data. The dependence of the collisional stopping power of dense matter on the beam density is illustrated. Finally, the Ohmic effect is discussed and, together with the proximity effect, incorporated into the beam-density effect.

## II. EXPERIMENTAL RESULTS

The experiment of proton beam energy loss in matter was carried out at the XG-III laser facility of Laser Fusion Research Center in Mianyang. Figure 1 shows the schematic set-up of the experimental arrangement. A beam consisting of protons ( $H^{1+}$ ) and carbon ions with different charge states (mostly  $C^{1+}$ ,  $C^{2+}$ ,  $C^{3+}$ , and  $C^{4+}$ ) is generated by a short and intense laser incident on a CH-coated tungsten foil (15- $\mu\text{m}$  thick). The laser beam has a duration of 800 fs, focal spot of 20  $\mu\text{m}$ , and total energy of 150 J. Due to the target normal sheath acceleration (TNSA) mechanism, the mixed beam originates from the rear side of the target with a relative wide spectrum for each kind of the ions. In order to achieve a quasi-monoenergetic beam we used a 500- $\mu\text{m}$  entrance slit, a magnetic dipole, and another 500- $\mu\text{m}$  exit slit to select ions according to their momentum ( $p$ ) to charge ( $q$ ) ratio  $p/q$ .

Protons are the first to arrive at the dipole, since their charge-to-mass ratio is the highest. The  $C^{4+}$  ion pulse trails the protons by 30 ns, followed by  $C^{3+}$ ,  $C^{2+}$ , and  $C^{1+}$ , which are delayed even more. After the dipole, ions of different species and charge states are separated, and the selected beam pulses are considered quasi-monoenergetic. The production and selection of beam particles ensure that the proton pulse is ahead of carbon pulses and the stopping of protons in the target is unaffected by subsequent carbon ions.

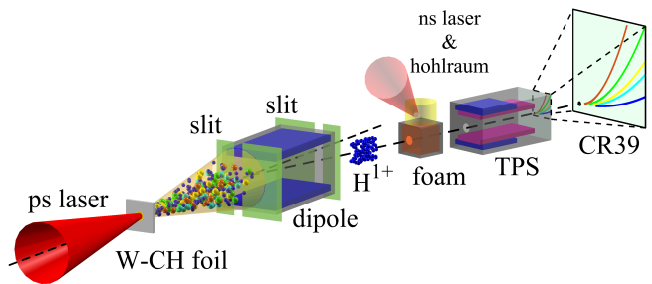


FIG. 1. Schematic set-up of the experimental arrangement including the production of beam particles by TNSA, the selection of quasi-monoenergetic ions, the transport region, and the diagnostic part.

The target of the experiment is a 1-mm-thick  $C_9H_{16}O_8$  foam of  $2 \text{ mg/cm}^3$  density behind a 1-mm aperture. Placed next to the foam is a gold hohlraum converter, which can generate soft X-rays by irradiating the hohlraum walls with a ns laser pulse (150 J). The soft X-rays then heats the foam and generates homogeneous, ns-long-living, and quasi-static ionized matter. In this way, the influence of electromagnetic fields from the foam heating on beam particles can be ignored. This method of plasma generation has been very well investigated [41–43]. By turning the ns laser on or off, one can decide whether it is plasma or a cold target. The following diagnostic part consists of a Thomson parabola spectrometer (TPS) [44–46] and a plastic track detector CR39, which is designed for energy measurement of charged particles. The electromagnetic fields of the TPS separate particles of different charge-to-mass ratios and energies. By analyzing the etched tracks on CR39, we obtain the spectra of particles.

For the proton beam we are interested in, its normalized energy distributions through vacuum and a cold target are shown in Fig. 2. At an initial injected energy of  $E = 3.36 \text{ MeV}$ , the TPS resolution is  $E/\delta E \sim 34$ , where  $\delta E$  is the energy range covered by the detected beam spot on the CR39. The full width at half maximum (FWHM) of the injected beam is 0.10 MeV. The central energy of the output beam after a cold target is 3.16 MeV, with the FWHM of 0.39 MeV. Experiment shows an energy loss of 0.20 MeV over 1 mm, which is one order of magnitude higher than the theoretical result of 0.021 MeV/mm calculated by Bethe formula [12, 13].

In previous work [38], a high degree of proton stopping was observed in plasma as shown in Fig. 2. The theoretical stopping power of the  $C_9H_{16}O_8$  plasma target with ionization degree of 0.64 ( $n_e = 4 \times 10^{20} \text{ cm}^{-3}$ ) for 3.36-MeV protons is 0.032 MeV/mm calculated by Bethe formula, with a free electron contribution around 84%. However, after the beam-plasma interaction, the experimental central energy of the output beam is 2.98 MeV, with a FWHM of 0.25 MeV. This large energy loss of 0.38 MeV/mm was attributed to the strong decelerating electric field caused by the beam-driven return current. PIC simulations indicate that the intensity of this decelerating electric field approaches 1 GV/m. However, the electron density of the cold target is much lower than that of the plasma, and is usually even smaller than the beam density.

The corresponding return current is not strong enough to neutralize the beam current or induce the decelerating electric field and therefore can almost be neglected. A different mechanism is required to explain the energy loss enhancement in the cold target.

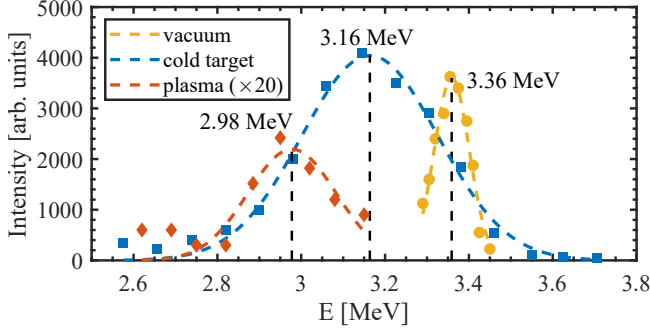


FIG. 2. Energy spectra of the proton particles through vacuum, a cold target, and plasma measured in experiments. The intensity through plasma is magnified 20 times.

### III. BEAM-DENSITY EFFECT ON ENERGY LOSS PROPOSED BY MCCORKLE AND IAFRATE

The beam-density effect, considered by McCorkle and Iafrate [35], refers to the stopping power enhancement of a dense ion beam in matter, which can reach orders of magnitude when compared to the stopping power of independent particles. This effect is closely related to the collective behavior of the dense beam, where neighboring ions jointly influence the interaction in a coherent way which is called the proximity effect in this paper. To be more specific, the enhanced collisional stopping power for a beam of density  $n_b$  in matter is

$$\begin{aligned} S_c &= S_0 + S_p \\ &= S_0 \left[ 1 + \int_0^\infty g(r/a) 4\pi r^2 n_b dr \right] \\ &\approx S_0 (1 + 2\pi n_b a^3 / 3) \\ &= S_0 (1 + N_c), \end{aligned} \quad (1)$$

where  $S_0$  is the single-particle stopping power,  $S_p$  is the stopping power resulting from the proximity effect, and  $a \equiv v/\omega_p$ . Here,  $v$  is the speed of beam particles,  $\omega_p = (4\pi n_{fe} e^2 / m_e)^{1/2}$  is the electron plasma frequency,  $n_{fe}$  is the free electron density,  $m_e$  is the electron mass. The interference term  $g(r/a)$  reflects the influence of neighboring beam particles and is specified by

$$g(r/a) \approx \begin{cases} 1/2, & r \leq a; \\ 0, & r > a. \end{cases} \quad (2)$$

The quantity  $2\pi n_b a^3 / 3$  is referred to as the cooperation number  $N_c$ , which reflects the degree of the proximity effect.

The total collisional stopping power is comprised of the single-particle part  $S_0$  and the part  $S_p$  arising from the proximity effect. For intense ion beams,  $S_p$  can be by far larger than  $S_0$ .

### IV. MODIFICATION OF BEAM-DENSITY EFFECT THEORY IN COLD TARGETS

#### A. Introducing local ionization degree into beam-density effect theory for cold targets

It should be noted that the above theory ignores the influence of possible decelerating electric field caused by the beam-driven return current, and underestimates the stopping power in plasma when compared with experimental results (see Appendix A for details). Nevertheless, the corresponding formula Eq. (1) can still be applied to plasma condition in order to estimate its collisional stopping power enhanced by the proximity effect. In the cold target, there are much less free electrons for the neutralization of beam particles. Taking a small value near zero as the free electron density when calculating the values of  $a$  and the cooperation number  $N_c$  leads to an abnormally high beam-density effect (see Appendix B for details). To explain the beam-density effect in cold targets and estimate its energy loss enhancement, ionization of the cold targets by intense ion beams must be considered.

Theoretically, protons with energy larger than the binding energy of bound electrons can excite bound target electrons to higher orbits and even ionize them, especially the valence electrons with low binding energy. In cold targets, nearly all the free electrons arise from the ionization by protons and these ionized electrons must be considered. The density of local ionized free electrons is  $n_{lfe} = \alpha_l n_{te}$ , where  $\alpha_l$  is the local ionization degree,  $n_{te}$  is the total electron density. These electrons lead to  $\omega_p = (4\pi n_{lfe} e^2 / m_e)^{1/2}$  and can contribute to the interference term in Eq. (2) by influencing the value of  $a = v/\omega_p$ . For the  $C_9H_{16}O_8$  target in the experiment, the total electron density is  $n_{te} = 6.4 \times 10^{20} \text{ cm}^{-3}$ . Additionally, the bound electrons represent a large fraction of the total electrons. Their resonance frequency is related to the ionization energy  $\omega_k = I_k/\hbar$ . By summing up the contributions of free electrons  $S_{fe}$  and bound electrons  $S_{be}$ , the total collisional stopping power for a dense beam in matter is rewritten as

$$\begin{aligned} S_c &= S_{fe} + S_{be} \\ &= S_{f0} \left[ 1 + \frac{2}{3} \pi n_b \left( \frac{v}{\omega_p} \right)^3 \right] + \sum_k S_{b0k} \left[ 1 + \frac{2}{3} \pi n_b \left( \frac{v}{\omega_k} \right)^3 \right] \\ &= \left( S_{f0} + \sum_k S_{b0k} \right) + \left[ S_{f0} \frac{n_b}{12\sqrt{\pi}} \left( \frac{m_e v^2}{\alpha_l n_{te} e^2} \right)^{3/2} \right. \\ &\quad \left. + \sum_k S_{b0k} \cdot \frac{2}{3} \pi n_b \left( \frac{v}{I_k/\hbar} \right)^3 \right] \\ &= S_0 + S_p. \end{aligned} \quad (3)$$

Here  $S_{f0}$  and  $S_{b0k}$  are the stopping power for an individual proton resulting from free electrons and bound electrons, respectively. According to Bethe formula [12, 13] with thermal correction [47], they are the components of  $S_0$  and can be specified by

$$S_{f0} = \frac{4\pi e^4 Z^2}{m_e v^2} G\left(\frac{v}{v_{th}}\right) n_{ife} \ln\left(\frac{2m_e v^2}{\hbar\omega_p}\right), \quad (4)$$

$$S_{b0k} = \frac{4\pi e^4 Z^2}{m_e v^2} n_{bek} \ln\left(\frac{2m_e v^2}{I_k}\right). \quad (5)$$

Here,  $Z$  is the effective charge state of injected ion beams,  $n_{ife}$  and  $n_{bek}$  are the densities of free and bound electrons.  $G(x) = \text{erf}(\sqrt{x}) - 2\sqrt{x/\pi} \exp(-x)$  is the Chandrasekhar thermal correction factor, which approaches 1 when  $x \gg 1$ .

### B. Determining local ionization degree through cross sections

The ionization of bound electrons in cold targets does also depend on the beam density. In order to determine their contribution to  $S_c(n_b)$ , the cross section for the target ionization by protons needs to be investigated.

By incorporating several adjustments into the plane-wave Born approximation (PWBA) [48, 49] theory, including approximation of the perturbed stationary state (PSS) and corrections for energy loss (E), Coulomb deflection (C), and relativistic (R) effects, Brandt and Lapicki [50, 51] proposed the ECPSSR theory, which has proven to be one of the most successful theories for evaluating cross sections of  $K$ - and  $L$ -shell ionization for ion impact on targets. Here, a versatile and fast program developed by Liu and Cipolla, ISICS [52, 53], is used to calculate ionization cross sections based on ECPSSR theory. The output cross sections for  $K$ - and  $L$ -shell ionization in H, C, O atoms by 3.36-MeV protons are shown in Table I.

TABLE I.  $K$ - and  $L$ -shell ionization cross sections of H, C, O atoms in barns (1 barn =  $10^{-24}$  cm<sup>2</sup>) for 3.36-MeV protons calculated by ISICS.

Elements	$\sigma_K$	$\sigma_{L_1}$	$\sigma_{L_2}$	$\sigma_{L_3}$
H	$1.384 \times 10^7$			
C	$4.904 \times 10^5$		$1.384 \times 10^7$	$8.484 \times 10^7$
O	$1.929 \times 10^5$	$8.778 \times 10^6$	$1.968 \times 10^8$	$3.937 \times 10^8$

The number of electrons ionized by the impact of a proton on a cold target of length  $d$  is specified by

$$N_{ie} = \left( \sum_k \sigma_k n_k \right) d, \quad (6)$$

where  $n_k$  is the number density of electrons with cross section of  $\sigma_k$ . For a proton beam with radius  $r = 0.5$  mm and beam length  $L = 25$   $\mu$ m, the number of protons contained in this

range is  $n_b \pi r^2 L$ . The local ionization degree  $\alpha_l$  is related to cross sections by

$$\alpha_l = \frac{N_{ie} (n_b \pi r^2 L)}{n_{te} \pi r^2 d} = \left( \sum_k \sigma_k n_k \right) \frac{n_b}{n_{te}} L. \quad (7)$$

Substituting the data of Table I into Eq. (7) yields the local ionization degree of the C<sub>9</sub>H<sub>16</sub>O<sub>8</sub> foam

$$\alpha_l \approx 6.35 \times 10^{-19} n_b \text{ (cm}^{-3}\text{)}. \quad (8)$$

The local ionization degree defined by Eq. (8) is the minimum value when ionization cross sections of all atoms are considered. In this way, the stopping power divergence (explosion) at low ionization degrees is eliminated.

### V. CALCULATING THE TOTAL STOPPING POWER

Substituting Eqs. (4), (5) and (8) into Eq. (3) yields  $S_0$ ,  $S_p$ , and the total collisional stopping power  $S$  of the cold target as functions of only the beam density  $n_b$ , as displayed in Fig. 3(a). When the beam density rises from  $10^{12}$  to  $10^{18}$  cm<sup>-3</sup>, the local ionization degree increases linearly from  $6.35 \times 10^{-7}$  to 0.635. At a low beam density, the beam-density effect is weak and the stopping power is mostly given by the single-particle result. When the beam density rises, the stopping power caused by the proximity effect increases sharply. It becomes comparable to the individual particle stopping power around the beam density of  $6 \times 10^{14}$  cm<sup>-3</sup>, and accounts for nearly 90% of  $S = 0.19$  MeV/mm at  $n_b = 5.5 \times 10^{16}$  cm<sup>-3</sup>, which is of the same order of density as the simulation estimation [38].

Considering a plasma target, what must be considered is the Ohmic stopping power  $S_{ohm} = ZeE$ , where  $E = \eta J$ ,  $\eta$  is the resistivity and  $J$  is the return current according to Ohm's law. The resistivity here is higher than the classical value of  $\eta_c = m_e v_{ei} / n_{fe} e^2$ , where the classical electron-ion collision frequency is specified by

$$v_{ei} = \frac{\pi Z_i^2 n_i e^4 \ln \Lambda}{m_e^{1/2} T_e^{3/2}}, \quad (9)$$

where  $Z_i$  is the ionization charge state of background plasmas,  $\ln \Lambda$  is the coulomb logarithm and  $T_e$  is the plasma temperature. This is because the collision between electrons and injected ions also needs to be considered for the resistivity calculation. According to the theory of wave-particle nonlinear interactions by Sagdeev and Galeev [54], the collision frequency between electrons and the beam is

$$v_{eb} = \omega_p \frac{v}{\sqrt{T_e/m_e}} \frac{T_b}{T_e}, \quad (10)$$

where the ion beam temperature (average thermal energy)  $T_b \approx 18$  eV in our case (see Appendix C for details). The final resistivity is then written as  $\eta = m_e (v_{ei} + v_{eb}) / n_{fe} e^2$ .

As shown in Fig. 3(b), the total stopping power in plasma at high beam densities is mainly composed of the Ohmic



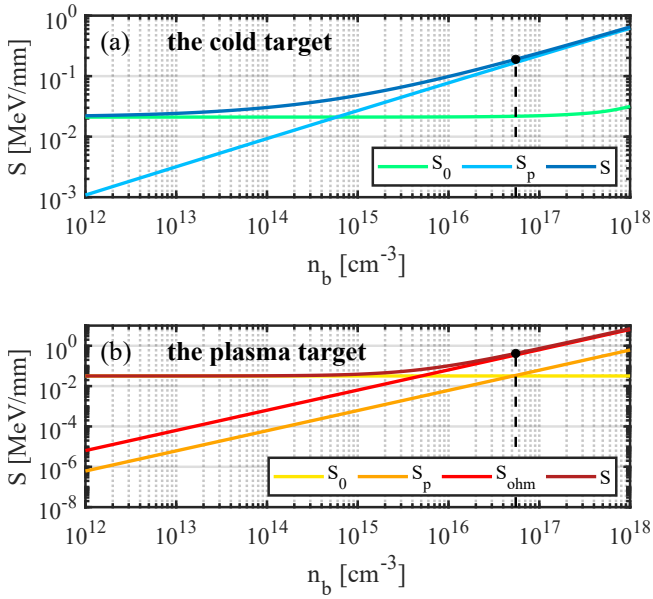


FIG. 3. Calculated stopping power as functions of the proton beam density for (a) a cold target and (b) plasma. At a high beam density,  $S_p$  is prominent for the cold target, while  $S_{ohm}$  makes up most of the stopping power for plasma.

stopping power  $S_{ohm}$ , with a resistivity  $\eta$  of 0.16  $\Omega$ -cm. At a beam density of  $5.5 \times 10^{16} \text{ cm}^{-3}$ , it reaches 0.42 MeV/mm, which is close to the experimental result of 0.38 MeV/mm.

The beam-density effect is an overall collective phenomenon caused by the high number of injected beam particles. It illustrates that the energy loss of intense ion beams in dense matter is composed of individual particle energy loss  $S_0$ , enhanced collisional energy loss  $S_p$ , which results from proximity effect of beam particles, and Ohmic energy loss  $S_{ohm}$ , written as  $S = S_0 + S_p + S_{ohm}$ . Usually only one of them may be dominant in specific scenarios. If there are few free electrons for neutralization of the beam, the beam-density effect may take the form of proximity effect, and the enhanced collisional energy loss is prominent [35]. If the return current is strong in plasmas with numerous free electrons, one may put the influence of decelerating electric field (Ohmic field) first [38].

The beam-density effect proposes new requirements for ion-driven warm dense matter (WDM) and fast ignition. The traditional relation between the stopping power and the beam energy can become unreliable for intense ion beams. Figure 4(a) plots the calculated proton stopping power in solid aluminum as a function of proton energy for beam densities of  $10^{12}$ ,  $10^{16}$ ,  $10^{17}$ , and  $10^{18} \text{ cm}^{-3}$ . There are so many free electrons in solid aluminum that the Ohmic stopping power  $S_{ohm}$  is responsible for the stopping power enhancement in this case. Correspondingly, the Bragg peaks of proton energy deposition with initial energy of 15 MeV are shown in Fig. 4(b). The beam-density effect can greatly affect the particle deposition in dense matter.

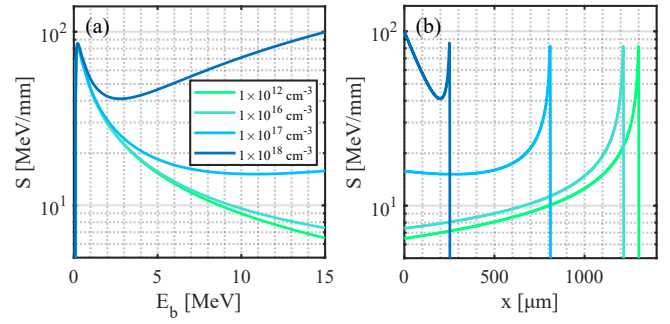


FIG. 4. (a) The calculated proton stopping power in solid aluminum as a function of proton energy with different beam densities, and (b) the corresponding Bragg curves of 15-MeV protons.

## VI. CONCLUSIONS

To sum up, a stopping power enhancement of one order of magnitude for an intense proton beam in a cold target was measured. The observed effect is attributed to the proximity effect. Here, a new method for numerically calculating the collisional stopping power for intense ion beams in dense matter is introduced. It modifies the beam-density effect theory with the local ionization caused by the intense beam. By obtaining the ionization cross sections of the cold target and considering Ohmic energy loss, the total stopping power is determined as a function of the beam density. To reach the energy loss of 0.20 MeV over 1 mm in the experiment, our method gives a beam density of  $5.5 \times 10^{16} \text{ cm}^{-3}$ , which agrees with the simulation estimation. The energy loss of intense ion beams in dense matter is composed of individual particle energy loss, enhanced collisional energy loss, which results from proximity effect of beam particles, and Ohmic energy loss. This research provides a new perspective to theoretically calculate the dramatic stopping power enhancement of intense ion beams in dense matter, and proposes new requirements for ICF and high-energy-density physics.

## DATA AVAILABILITY

The data that support the findings of this study are available from the corresponding author upon reasonable request.

## ACKNOWLEDGMENTS

This work was supported by National Key R&D Program of China (Grant No. 2019YFA0404900), Science Challenge Project (Grant No. TZ2016005), National Natural Science Foundation of China (Grants No. U2030104, No. 11705141, No. 11775282, No. 11605269, and No. U1532263), China Postdoctoral Science Foundation (Grants No. 2017M623145 and No. 2018M643613), and Science and Technology on Plasma Physics Laboratory (Grant No. J202108010).

## Appendix A: Collisional stopping power for a proton beam in plasma by the beam-density theory

Fig. 5 shows the collisional stopping power  $S_c$  for a 3.36-MeV proton beam in the plasma of the experiment as a function of the beam density by Eq. (3), and compares the results with simulations. The modified collisional stopping power  $S_c$  is composed of the free electron contribution  $S_{fe}$  and the bound electron contribution  $S_{be}$ . The latter only takes a small percentage and can be regarded as a constant ( $\sim 4.9$  keV/mm). It is the increase of  $S_{fe}$  that makes  $S_c$  rise sharply. When the beam density rises from  $10^{12}$  to  $10^{18}$   $\text{cm}^{-3}$ , the collisional stopping power in the plasma can increase by one order of magnitude from 0.032 to over 0.6 MeV/mm. Simulations also verify the enhancement of beam energy loss [38]. In addition, to reach a stopping power of 0.38 MeV/mm as measured in the plasma of the experiment, simulations and the theory give beam densities of  $\sim 8 \times 10^{16}$  and  $5 \times 10^{17}$   $\text{cm}^{-3}$ , respectively. The beam-density theory apparently underestimates the enhancement of the stopping power in plasma. This is because it calculates the collisional energy loss enhancement resulting from proximity of beam ions, but ignores the impact of the decelerating electric field caused by the beam-driven return current, which is the main reason for the enhanced energy loss in plasma case.

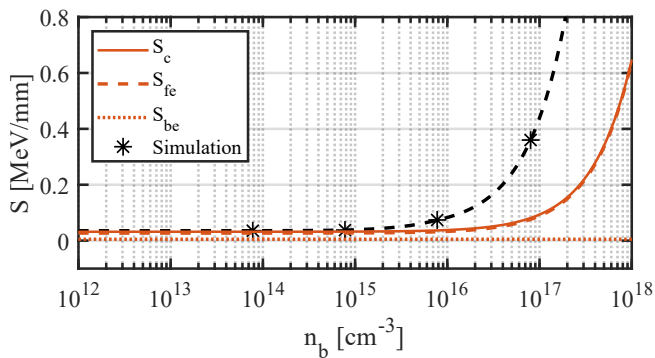


FIG. 5. Several stopping powers for proton beams with densities  $10^{12}$ – $10^{18}$   $\text{cm}^{-3}$  in the plasma of the experiment. The initial beam energy is 3.36 MeV. The curves of  $S_c$ ,  $S_{fe}$  and  $S_{be}$  are outputs of Eq. (3). Several simulation results are also presented.

## Appendix B: Problems of explosive stopping power increase at low electron densities

Applying the beam-density effect theory of McCorkle and Iafrate [35] requires free electrons of certain density existing in matter. Otherwise the plasma frequency  $\omega_p$  would be very small for an electron density  $n_{fe}$  near zero, leading to enormous values of  $a = v/\omega_p$  and cooperation number  $N_c$  and then the explosion of the stopping power  $S_c$ .

Fig. 6 shows this unphysical energy loss increase of dense proton beam in cold targets and low-density plasma by the beam-density effect theory. In Fig. 6(a), the stopping power of the  $\text{C}_9\text{H}_{16}\text{O}_8$  target with mass density  $\rho_t = 2$   $\text{mg}/\text{cm}^3$  and

ionization degree  $\alpha$  varying from  $10^{-3}$  to 1 (fully ionized) for a single proton  $S_0$  (blue) and a proton beam  $S_c$  (red) with density  $n_b = 8 \times 10^{16}$   $\text{cm}^{-3}$  is presented. The initial beam energy is  $E = 3.36$  MeV. The energy loss result of the proton beam is based on the original beam-density effect theory and is obtained by Eq. (1). The local ionization is not considered here. Note that two curves are shown with different y axes and the stopping power with beam-density effect is orders of magnitude higher than that for a single particle. Marked dots in Figs. 6 show the results corresponding to the experimental plasma with temperature 17 eV and ionization degree 0.64.

When the target evolves from plasma to a cold target with the ionization degree  $\alpha$  declining from 0.64 to 0.001, though the single-particle stopping power  $S_0$  decreases from 0.032 to 0.021 MeV/mm, the total collisional stopping power increases dramatically from 0.090 to  $6 \times 10^2$  MeV/mm according to Eq. (1). This enhancement of stopping power is far more larger than the experimental result of 0.20 MeV/mm in cold targets. Because 1) an ionization degree of  $10^{-3}$  is lower than the actual value and 2) both free and bound electron contributions  $S_0$  multiply the same cooperation number  $2\pi n_b (v/\omega_p)^3/3$  while the bound electron part should be excluded and time a smaller cooperation number  $2\pi n_b (v/\omega_k)^3/3$ . By calculating the minimum local ionization degree using ionization cross sections in Eq. (8), the corresponding collisional stopping power is computed as two parts in Eq. (3). In this way, the stopping power explosion is eliminated.

Fig. 6(b) displays  $S_0$  and  $S_c$  of the  $\text{C}_9\text{H}_{16}\text{O}_8$  target with fixed ionization degree 0.64 (same as the plasma target in the experiment) and mass density  $\rho_t$  from 0.002 to 200  $\text{mg}/\text{cm}^3$ . Reducing the target density can also make the electron density of the target decline. If Eq. (1) of the beam-density effect theory is applied to low-density plasma, the stopping power would be abnormally enormous and obviously unphysical. In fact, when the electron density is lower than the beam density, the polarization wakes produced by the beam particles is weak, and so is the collective effect of the beam particles. The lower the target density is, the closer the stopping power to the single-particle case. Simulation results also show the tendency of falling as the target density decreases in the range of  $\rho_t < 0.2$   $\text{mg}/\text{cm}^3$ . It is under the condition that the total electron density  $n_{te}$  of the target is higher than the beam density  $n_b$  that we consider using the beam-density effect theory to calculate the enhanced collisional stopping power.

## Appendix C: Ion beam temperature estimation

The ion beam temperature  $T_b$  discussed here refers to the average thermal energy of injected protons, which excludes the initial kinetic energy of  $E = 3.36$  MeV. It mainly results from beam divergence and is restricted to the width of the slit  $d'$  behind the dipole and the aperture  $d$  in front of the target (see Fig. 1). Polar coordinates  $(r', \theta')$  and  $(r, \theta)$  are used in planes of the slit (plane I) and the target aperture (plane II), respectively. Only protons with  $r'$  smaller than  $d'/2$  are considered to make the system axisymmetric for simplicity.

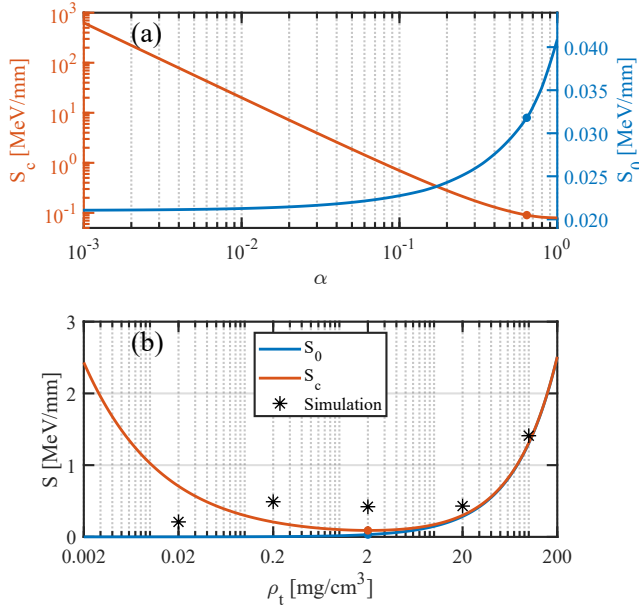


FIG. 6. Explosive stopping power increase of targets with different ionization degrees and different mass densities. The blue and red curves are results for a single proton and for a dense beam with density  $n_b = 8 \times 10^{16} \text{ cm}^{-3}$ , respectively. (a) The target has mass density  $2 \text{ mg/cm}^3$  and ionization degree varying from  $10^{-3}$  to 1 (fully ionized). (b) The target has the same ionization degree with the experiment target of 0.64. The mass density of the target varies from 0.002 to  $200 \text{ mg/cm}^3$ . The initial energy of both the individual particle and the dense beam is 3.36 MeV. Marked dots are the results corresponding to the experiment.

The area density functions of protons in plane I and plane II are  $g(r')$  and  $f(r)$ . The distance between plane I and plane II is  $L$ . The average thermal energy is specified by

$$T_b = \frac{\int_0^{2\pi} \int_0^{d/2} \frac{1}{2} m_p \overline{v_t^2} f(r) r dr d\theta}{\int_0^{2\pi} \int_0^{d/2} f(r) r dr d\theta}, \quad (\text{C1})$$

where  $m_p$  is the proton mass,

$$\overline{v_t^2}(r, \theta) = \frac{\int_0^{2\pi} \int_0^{d/2} v_t^2 g(r') r' dr' d\theta'}{\int_0^{2\pi} \int_0^{d/2} g(r') r' dr' d\theta'}, \quad (\text{C2})$$

$v_t = vl/L$  is the transverse velocity,  $v = \sqrt{2E/m_p}$  and  $l = \sqrt{r^2 + r'^2 - 2rr' \cos(\theta - \theta')}$  is the transverse distance between  $(r', \theta')$  and  $(r, \theta)$ .

In the experiment,  $d' = 0.5 \text{ mm}$ ,  $d = 1 \text{ mm}$ ,  $L = 17 \text{ cm}$ . Considering  $f(r)$  and  $g(r')$  as two constant functions, one obtains  $T_b \approx 18 \text{ eV}$ . If Gaussian distribution is applied,  $f(r) = A \exp(-r^2/2\sigma^2)$  and  $g(r') = A' \exp(-r'^2/2\sigma'^2)$ , where  $\sigma = d/2\sqrt{2\ln 2}$  and  $\sigma' = d'/2\sqrt{2\ln 2}$ . The according beam temperature is about 16 eV. Since the plasma temperature  $T_e$  is 17 eV, it can be assumed that  $T_b \approx T_e$  in our experimental condition.

- 
- [1] C. K. Li and R. D. Petrasso, *Charged-Particle Stopping Powers in Inertial Confinement Fusion Plasmas*, Phys. Rev. Lett. 70, 3059 (1993).
- [2] C. K. Li and R. D. Petrasso, *Energy Deposition of MeV Electrons in Compressed Targets of Fast-Ignition Inertial Confinement Fusion*, Phys. Plasmas 13, 056314 (2006).
- [3] O. A. Hurricane, D. A. Callahan, D. T. Casey, E. L. Dewald, T. R. Dittrich, T. Doppner, S. Haan, D. E. Hinkel, L. F. B. Hopkins, O. Jones, A. L. Kritcher, S. Le Pape, T. Ma, A. G. MacPhee, J. L. Milovich, J. Moody, A. Pak, H. S. Park, P. K. Patel, J. E. Ralph, H. F. Robey, J. S. Ross, J. D. Salmonson, B. K. Spears, P. T. Springer, R. Tommasini, F. Albert, L. R. Benedetti, R. Bionta, E. Bond, D. K. Bradley, J. Caggiano, P. M. Celliers, C. Cerjan, J. A. Church, R. Dylla-Spears, D. Edgell, M. J. Edwards, D. Fittinghoff, M. A. B. Garcia, A. Hamza, R. Hatarik, H. Herrmann, M. Hohenberger, D. Hoover, J. L. Kline, G. Kyrala, B. Koziolowski, G. Grim, J. E. Field, J. Frenje, N. Izumi, M. G. Johnson, S. F. Khan, J. Kruer, T. Kohut, O. Landen, F. Merrill, P. Michel, A. Moore, S. R. Nagel, A. Nikroo, T. Parham, R. R. Rygg, D. Sayre, M. Schneider, D. Shaughnessy, D. Strozzi, R. P. J. Town, D. Turnbull, P. Volegov, A. Wan, K. Widmann, C. Wilde, and C. Yeamans, *Inertially Confined Fusion Plasmas Dominated by Alpha-Particle Self-Heating*, Nat. Phys. 12, 800 (2016).
- [4] M. Durante and J. S. Loeffler, *Charged Particles in Radiation Oncology*, Nat. Rev. Clin. Oncol. 7, 37 (2010).
- [5] T. Rackwitz and J. Debus, *Clinical Applications of Proton and Carbon Ion Therapy*, Semin. Oncol. 46, 226 (2019).
- [6] A. Spitkovsky, *On the Structure of Relativistic Collisionless Shocks in Electron-Ion Plasmas*, Astrophys. J. Lett. 673, L39 (2008).
- [7] C. M. Huntington, F. Fiuza, J. S. Ross, A. B. Zylstra, R. P. Drake, D. H. Froula, G. Gregori, N. L. Kugland, C. C. Kuranz, M. C. Levy, C. K. Li, J. Meinecke, T. Morita, R. Petrasso, C. Plechaty, B. A. Remington, D. D. Ryutov, Y. Sakawa, A. Spitkovsky, H. Takabe, and H. S. Park, *Observation of Magnetic Field Generation via the Weibel Instability in Interpenetrating Plasma Flows*, Nat. Phys. 11, 173 (2015).
- [8] D. Bohne, I. Hofmann, G. Kessler, G. L. Kulcinski, J. Meyerter-Vehn, U. Vonmollendorff, G. A. Moses, R. W. Muller, I. N. Sviatoslavsky, D. K. Sze, and W. Vogelsang, *HIBALL-A Conceptual Design Study of a Heavy-Ion Driven Inertial Confinement Fusion Power-Plant*, Nucl. Eng. Des. 73, 195 (1982).
- [9] I. Hofmann, *Review of Accelerator Driven Heavy Ion Nuclear Fusion*, Matter Radiat. Extremes 3, 1 (2018).
- [10] G. Sarri, C. A. Cecchetti, L. Romagnani, C. M. Brown, D. J. Hoarty, S. James, J. Morton, M. E. Dieckmann, R. Jung, O. Willi, S. V. Bulanov, F. Pegoraro, and M. Borghesi, *The Application of Laser-Driven Proton Beams to the Radiography of Intense Laser-Hohlraum Interactions*, New J. Phys. 12, 045006(2010).

- [11] S. Y. Gus'kov, *Fast Ignition of Inertial Confinement Fusion Targets*, Plasma Phys. Rep. 39, 1 (2013).
- [12] H. Bethe, *Zur Theorie des Durchgangs schneller Korpuskularstrahlen durch Materie*, Ann. Phys. 397, 325 (1930).
- [13] H. Bethe, *About the Side Radiation and the Nature of the Coloring Matter in Natural Blue Halite*, Z. Phys. 76, 293 (1932).
- [14] F. Bloch, *Zur Bremsung rasch bewegter Teilchen beim Durchgang durch Materie*, Ann. Phys. 408, 285 (1933).
- [15] C. K. Li and R. D. Petrasso, *Fokker-Planck Equation for Moderately Coupled Plasmas*, Phys. Rev. Lett. 70, 3063 (1993).
- [16] C. Deutsch and G. Maynard, *Ion Stopping in Dense Plasmas: a Basic Physics Approach*, Matter Radiat. Extremes 1, 277 (2016).
- [17] L. S. Brown, D. L. Preston, and R. L. Singleton, *Charged Particle Motion in a Highly Ionized Plasma*, Phys. Rep. 410, 237 (2005).
- [18] D. O. Gericke, *Stopping Power for Strong Beam-Plasma Coupling*, Laser Part. Beams 20, 471 (2002).
- [19] J. A. Frenje, R. Florido, R. Mancini, T. Nagayama, P. E. Grabowski, H. Rinderknecht, H. Sio, A. Zylstra, M. G. Johnson, C. K. Li, F. H. Seguin, R. D. Petrasso, V. Y. Glebov, and S. P. Regan, *Experimental Validation of Low-Z Ion-Stopping Formalisms around the Bragg Peak in High-Energy-Density Plasmas*, Phys. Rev. Lett. 122, 015002 (2019).
- [20] A. B. Zylstra, J. A. Frenje, P. E. Grabowski, C. K. Li, G. W. Collins, P. Fitzsimmons, S. Glenzer, F. Graziani, S. B. Hansen, S. X. Hu, M. G. Johnson, P. Keiter, H. Reynolds, J. R. Rygg, F. H. Seguin, and R. D. Petrasso, *Measurement of Charged-Particle Stopping in Warm Dense Plasma*, Phys. Rev. Lett. 114, 215002 (2015).
- [21] W. Cayzac, A. Frank, A. Ortner, V. Bagnoud, M. M. Basko, S. Bedacht, C. Blaser, A. Blazevic, S. Busold, O. Deppert, J. Ding, M. Ehret, P. Fiala, S. Frydrych, D. O. Gericke, L. Hallo, J. Helfrich, D. Jahn, E. Kjartansson, A. Knetsch, D. Kraus, G. Malka, N. W. Neumann, K. Pepitone, D. Pepler, S. Sander, G. Schaumann, T. Schlegel, N. Schroeter, D. Schumacher, M. Seibert, A. Tauschwitz, J. Vorberger, F. Wagner, S. Weih, Y. Zobus, and M. Roth, *Experimental Discrimination of Ion Stopping Models near the Bragg Peak in Highly Ionized Matter*, Nat. Commun. 8, 15693 (2017).
- [22] W. Brandt, A. Ratkowski, and R. H. Ritchie, *Energy-Loss of Swift Proton Clusters in Solids*, Phys. Rev. Lett. 33, 1325 (1974).
- [23] W. Brandt and R. H. Ritchie, *Penetration of Swift Ion Clusters through Solids*, Nucl. Instrum. Meth. 132, 43 (1976).
- [24] T. Marinkovic, I. Radovic, D. Borcka, and Z. L. Miskovic, *Wake Effect in the Interaction of Slow Correlated Charges with Supported Graphene Due to Plasmon-Phonon Hybridization*, Phys. Lett. A 379, 377 (2015).
- [25] T. Nandi, K. Haris, Hala, G. Singh, P. Kumar, R. Kumar, S. K. Saini, S. A. Khan, A. Jhingan, P. Verma, A. Tauheed, D. Mehta, and H. G. Berry, *Fast Ion Surface Energy Loss and Straggling in the Surface Wake Fields*, Phys. Rev. Lett. 110, 163203 (2013).
- [26] V. Despoja, K. Dekanic, M. Sunjic, and L. Marusic, *Ab Initio Study of Energy Loss and Wake Potential in the Vicinity of a Graphene Monolayer*, Phys. Rev. B 86, 165419 (2012).
- [27] G. Basbas and R. H. Ritchie, *Vicinage Effects in Ion-Cluster Collisions with Condensed Matter and with Single Atoms*, Phys. Rev. A 25, 1943 (1982).
- [28] N. E. Koval, A. G. Borisov, L. F. S. Rosa, E. M. Stori, J. F. Dias, P. L. Grande, D. Sanchez-Portal, and R. Diez Muino, *Vicinage Effect in the Energy Loss of H<sub>2</sub> Dimers: Experiment and Calculations Based on Time-Dependent Density-Functional Theory*, Phys. Rev. A 95, 062707 (2017).
- [29] A. L'Hoir, C. Cohen, J. J. Ganem, I. Trimaille, I. C. Vickridge, and S. M. Shubeita, *Vicinage Effect for Hydrogen Clusters in Si<sub>3</sub>N<sub>4</sub> and SiO<sub>2</sub>*, Phys. Rev. A 85, 042901 (2012).
- [30] S. M. Shubeita, P. L. Grande, J. F. Dias, R. Garcia-Molina, C. D. Denton, and I. Abril, *Energy Loss of Swift H<sub>2</sub><sup>+</sup> and H<sub>3</sub><sup>+</sup> Molecules in Gold: Vicinage Effects*, Phys. Rev. B 83, 245423 (2011).
- [31] B. G. Logan, W. F. Dove, K. A. Geber, and G. C. Goldenbaum, *X-Ray Bremsstrahlung Measurements of an Intense Relativistic Electron Beam Propagating in a Plasma*, IEEE Trans. Plasma Sci. PS-2, 182 (1974).
- [32] G. Wallis, K. Sauer, D. Sunder, S. E. Rosinskii, A. A. Rukhadze, and V. G. Rukhlin, *Injection of High-Current Relativistic Electron Beams into Plasma and Gas*, Sov. Phys. Usp. 17, 492 (1975).
- [33] B. Vauzour, J. J. Santos, A. Debayle, S. Hulin, H. P. Schlenvoigt, X. Vaisseau, D. Batani, S. D. Baton, J. J. Honrubia, P. Nicolai, F. N. Beg, R. Benocci, S. Chawla, M. Coury, F. Dorchies, C. Fourment, E. d'Humieres, L. C. Jarrot, P. McKenna, Y. J. Rhee, V. T. Tikhonchuk, L. Volpe, and V. Yahia, *Relativistic High-Current Electron-Beam Stopping-Power Characterization in Solids and Plasmas: Collisional Versus Resistive Effects*, Phys. Rev. Lett. 109, 255002 (2012).
- [34] S. Y. Gus'kov and P. A. Kuchugov, *Resistivity Contribution to Stopping Power and Plasma Heating by Laser-Accelerated Electrons*, Phys. Plasmas 29, 122702 (2022).
- [35] R. A. McCorkle and G. J. Iafate, *Beam-Density Effect on the Stopping of Fast Charged Particles in Matter*, Phys. Rev. Lett. 39, 1263 (1977).
- [36] D. Wu, W. Yu, Y. T. Zhao, D. H. H. Hoffmann, S. Fritzsche, and X. T. He, *Particle-in-Cell Simulation of Transport and Energy Deposition of Intense Proton Beams in Solid-State Materials*, Phys. Rev. E 100, 013208 (2019).
- [37] B. Z. Chen, D. Wu, J. R. Ren, D. H. H. Hoffmann, and Y. T. Zhao, *Transport of Intense Particle Beams in Large-Scale Plasmas*, Phys. Rev. E 101, 051203(R) (2020).
- [38] J. R. Ren, Z. G. Deng, W. Qi, B. Z. Chen, B. B. Ma, X. Wang, S. Yin, J. H. Feng, W. Liu, Z. F. Xu, D. H. H. Hoffmann, S. Y. Wang, Q. P. Fan, B. Cui, S. K. He, Z. R. Cao, Z. Q. Zhao, L. F. Cao, Y. Q. Gu, S. P. Zhu, R. Cheng, X. M. Zhou, G. Q. Xiao, H. W. Zhao, Y. H. Zhang, Z. Zhang, Y. T. Li, D. Wu, W. M. Zhou, and Y. T. Zhao, *Observation of a High Degree of Stopping for Laser-Accelerated Intense Proton Beams in Dense Ionized Matter*, Nat. Commun. 11, 5157 (2020).
- [39] J. Kim, C. McGuffey, B. Qiao, M. S. Wei, P. E. Grabowski, and F. N. Beg, *Varying Stopping and Self-Focusing of Intense Proton Beams as They Heat Solid Density Matter*, Phys. Plasmas 23, 043104 (2016).
- [40] B. Z. Chen, D. Wu, J. R. Ren, J. L. Wang, and Y. T. Zhao, *Confinement of Intense Proton Beams by an Applied Axial Magnetic Field in Large-Scale Plasma*, Phys. Plasmas 29, 022303 (2022).
- [41] O. N. Rosmej, V. Bagnoud, U. Eisenbarth, V. Vatulín, N. Zhidkov, N. Suslov, A. Kunin, A. Pinegin, D. Schafer, T. Nisius, T. Wilhein, T. Rienecker, J. Wiechula, J. Jacoby, Y. Zhao, G. Vergunova, N. Borisenko, and N. Orlov, *Heating of Low-Density Cho-Foam Layers by Means of Soft X-Rays*, Nucl. Instrum. Methods Phys. Res., Sect. A 653, 52 (2011).
- [42] O. N. Rosmej, N. Suslov, D. Martsovenko, G. Vergunova, N. Borisenko, N. Orlov, T. Rienecker, D. Klir, K. Rezack, A. Orekhov, L. Borisenko, E. Krousky, M. Pfeifer, R. Dudzak, R. Maeder, M. Schaechinger, A. Schoenlein, S. Zaechter, J. Jacoby, J. Limpouch, J. Ullschmied, and N. Zhidkov, *The*



- Hydrodynamic and Radiative Properties of Low-Density Foams Heated by X-Rays*, Plasma Phys. Contr. Fusion 57, 094001 (2015).
- [43] S. Faik, A. Tauschwitz, M. M. Basko, J. A. Maruhn, O. Rosmej, T. Rienecker, V. G. Novikov, and A. S. Grushin, *Creation of a Homogeneous Plasma Column by Means of Hohlraum Radiation for Ion-Stopping Measurements*, High. Energy Density Phys. 10, 47 (2014).
- [44] Y. H. Zhang, Z. Zhang, B. J. Zhu, W. M. Jiang, L. Cheng, L. Zhao, X. P. Zhang, X. Zhao, X. H. Yuan, B. W. Tong, J. Y. Zhong, S. K. He, F. Lu, Y. C. Wu, W. M. Zhou, F. Q. Zhang, K. N. Zhou, N. Xie, Z. Huang, Y. Q. Gu, S. M. Wen, M. H. Xu, Y. J. Li, and Y. T. Li, *An Angular-Resolved Multi-Channel Thomson Parabola Spectrometer for Laser-Driven Ion Measurement*, Rev. Sci. Instrum. 89, 093302 (2018).
- [45] D. Jung, R. Horlein, D. Kiefer, S. Letzring, D. C. Gautier, U. Schramm, C. Hubsch, R. Ohm, B. J. Albright, J. C. Fernandez, D. Habs, and B. M. Hegelich, *Development of a High Resolution and High Dispersion Thomson Parabola*, Rev. Sci. Instrum. 82, 013306 (2011).
- [46] R. Rajeev, K. P. M. Rishad, T. M. Trivikram, V. Narayanan, and M. Krishnamurthy, *A Thomson Parabola Ion Imaging Spectrometer Designed to Probe Relativistic Intensity Ionization Dynamics of Nanoclusters*, Rev. Sci. Instrum. 82, 083303 (2011).
- [47] S. Chandrasekhar, *Stochastic Problems in Physics and Astronomy*, Rev. Mod. Phys. 15, 0001 (1943).
- [48] E. Merzbacher and H. W. Lewis, *X-Ray Production by Heavy Charged Particles*, in *Corpuscles and Radiation in Matter II*, Vol.34, edited by S. Flügge (Springer Berlin Heidelberg, Berlin, Heidelberg, 1958) pp.166–192.
- [49] O. Benka and A. Kropf, *Tables for Plane-Wave Born-Approximation Calculations of K-and L-Shell Ionization by Protons*, At. Data Nucl. Data Tables 22, 219 (1978).
- [50] W. Brandt and G. Lapicki, *L-Shell Coulomb Ionization by Heavy Charged-Particles*, Phys. Rev. A 20, 465 (1979).
- [51] W. Brandt and G. Lapicki, *Energy-Loss Effect in Inner-Shell Coulomb Ionization by Heavy Charged-Particles*, Phys. Rev. A 23, 1717 (1981).
- [52] Z. Q. Liu and S. J. Cipolla, *ISICS: a Program for Calculating K-, L-and M-Shell Cross Sections from ECPSR Theory Using a Personal Computer*, Comput. Phys. Commun. 97, 315 (1996).
- [53] M. Batic, M. G. Pia, and S. J. Cipolla, *Corrected ISICSoo Class Version*, Comput. Phys. Commun. 184, 2232 (2013).
- [54] R. Z. Sagdeev and A. A. Galeev, *Nonlinear Plasma Theory*, edited by T. M. O’Neil and D. L. Book (Benjamin, New York, 1969) p.94.